ACS Catalysis

Research Article

pubs.acs.org/acscatalysis

Who Is Doing the Job? Unraveling the Role of Ga_2O_3 in Methanol Steam Reforming on Pd_2Ga/Ga_2O_3

Andreas Haghofer,[†] Davide Ferri,[‡] Karin Föttinger,*[,†] and Günther Rupprechter[†]

[†]Institute of Materials Chemistry, Vienna University of Technology, Getreidemarkt 9/BC, A-1060 Vienna, Austria

[‡]Empa, Swiss Federal Laboratories for Material Science and Technology, Laboratory for Solid State Chemistry and Catalysis, Ueberlandstr. 129, CH-8600 Dübendorf, Switzerland

Supporting Information

ABSTRACT: A systematic study of the nature, stability, and dynamics of surface species present under methanol steam reforming (MSR) conditions over Pd/Ga_2O_3 and Pd_2Ga/Ga_2O_3 was performed by combining steady state and concentration modulation FTIR spectroscopy. This powerful combination allowed us to obtain novel mechanistic insights into the selective pathway leading to the formation of H_2 and CO_2 and thus to contribute to the understanding of the remarkably different catalytic properties of Pd/Ga_2O_3 and Pd_2Ga/Ga_2O_3. Strongly enhanced formation of adsorbed formates at low temperatures was detected on Pd_2Ga/Ga_2O_3. We ascribe the facilitated formation of these species to the presence of reactive oxygen sites in the Ga_2O_3 surface, which are formed during high-temperature reduction and formation of the intermetallic compound Pd_2Ga. While the stability of involved formates is high under reaction conditions of methanol decomposition (i.e., in the absence of H_2O), the entire adsorption system behaves more dynamically in the presence of water. We propose that the introduction of H_2O into the system converts stable bridging- and bidentate formates into more reactive, monodentate species. These react either with adsorbed methoxy to methyl formate (MFO) in the absence of water or with OH groups supplied by H_2O to CO_2 and H_2. The reaction with OH is faster, leading to a smaller concentration of intermediate monodentate formate under MSR conditions. MFO is easily decomposed into CO and CH_3OH and therefore, it is unlikely to be an intermediate in the selective MSR reaction to CO_2 and H_2. While the formation of intermetallic particles by high-temperature reduction is a prerequisite to achieving high MSR selectivity, our results suggest that the reaction sequence predominantly proceeds on the Ga_2O_3 surface, that is modified by the high temperature reduction and the formation of Pd_2Ga, and is only promoted by the presence of the intermetallic particles.

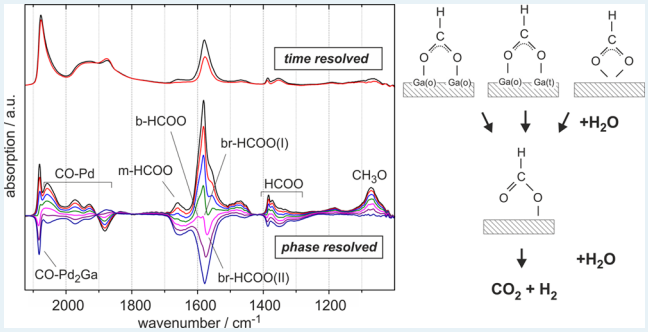

KEYWORDS: *palladium, gallium oxide, intermetallic compound, methanol steam reforming, methanol decomposition, in situ IR spectroscopy, concentration modulation, reaction mechanism, reaction intermediates*

1. INTRODUCTION

The utilization of hydrogen in proton exchange membrane (PEM) fuel cells offers a clean and efficient source of electricity for mobile applications. One possibility to circumvent the difficulties of transporting liquefied hydrogen is the use of a liquid fuel that is reformed into H_2 onboard.[1,2] For such applications the steam reforming of methanol (MSR) has been intensively studied.[3−5]

$$CH_3OH + H_2O \rightarrow CO_2 + 3H_2 \quad (1)$$

Selectivity of the reforming catalyst plays a crucial role in the overall system because of the sensitivity of downstream fuel cell anode electrocatalysts to carbon monoxide (CO), a common (by)product in the conversion of CH_3OH.[6] Traditionally, Cu-based catalysts employed in methanol synthesis have been used in MSR as well. However, because of their lack of long-term stability under MSR conditions,[7] alternative systems have emerged, most importantly Pd supported on the reducible oxides of Zn, Ga, and In. Iwasa and co-workers were the first to describe the remarkable catalytic properties of Pd on these supports in MSR[8] and ascribed it to the formation of an alloy between Pd and reduced Zn, Ga, and In from the support. For Pd−Ga systems this idea was more recently expanded by studies on the formation and stability of these alloys and the correlation between alloy phase and catalytic properties.[7,9−11] An important point that has been neglected in the literature until very recently[12] is the role of the oxidic support in the reaction mechanism versus that of the alloy particles. While for unsupported PdZn the steam reforming activity of pure alloy surfaces has been demonstrated,[13,14] there is experimental and

Special Issue: Operando and In Situ Studies of Catalysis

Received: July 18, 2012
Revised: August 29, 2012
Published: September 17, 2012

theoretical evidence that ZnO,[15] In_2O_3,[16] and at lower selectivity also Ga_2O_3[17] on their own (i.e., in the absence of Pd) can be MSR catalysts as well at higher reaction temperatures. In addition, the inability of purely intermetallic PdGa surfaces with no oxidic support to activate H_2O and therefore to be selective in MSR has recently been demonstrated.[12] For methanol synthesis, which is the reverse reaction of MSR, it has been proposed that carbonaceous reaction intermediates are adsorbed on the oxide support and Pd plays only the role of an atomic hydrogen source, that is, Pd accelerates the reaction in a bifunctional mechanism.[18]

At this point it should be mentioned that mechanistic aspects of methanol synthesis and steam reforming are still highly debated, even for Cu based catalysts which have been industrially applied for decades and have been the focus of a compelling number of experimental and theoretical studies (see refs 5,19−22 and references therein). The two most commonly discussed reaction mechanisms proceed (i) over methyl formate (i.e., the "methyl formate" or "dehydrogenation-hydrolysis" mechanism[19,23]), which is then hydrolyzed to adsorbed formate or formic acid or (ii) over methylenebisoxy directly to adsorbed formate.[21] In both cases the adsorbed formate/formic acid then decomposes primarily to CO_2 and H_2. For the more recently applied Pd−Zn, Pd−Ga, and Pd−In systems, very few mechanistic studies have been published.[21,24]

In this work a systematic study of the nature, stability, and dynamics of surface-adsorbed species was performed under a variety of reaction conditions. While the interaction of CH_3OH with Pd, as well as with Ga_2O_3 has been studied on model- and high performance systems in the past, there is no study so far dealing with the effect of intermetallic particles versus that of metallic particles (both supported on Ga_2O_3) on the evolution of surface adsorbed species in MSR. Aided by our recent thorough characterization of the formation and stability of intermetallic Pd−Ga particles supported on Ga_2O_3, this comparison can be expected to contribute to the understanding of the remarkably different catalytic properties of the two systems Pd/Ga_2O_3 and Pd_2Ga/Ga_2O_3. In situ concentration modulation FTIR spectroscopy enabled us to additionally derive information on the dynamic response of the spectroscopically observed surface species to changes in reaction conditions. This allowed us to differentiate potential reaction intermediates from mere spectator species and to propose a reaction mechanism of MSR on Pd_2Ga/Ga_2O_3.

2. EXPERIMENTAL SECTION

2.1. Materials and Characterization. The 2 wt % Pd/β-Ga_2O_3 catalyst was synthesized by incipient wetness impregnation of commercial β-Ga_2O_3 (Alfa Aesar, 99.99% purity, particle size <250 μm,) with a solution of palladium(II) acetate (Fluka) dissolved in toluene (Merck, p.a.). The surface area of the Ga_2O_3 support was 7 m^2/g determined by N_2 adsorption. X-ray photoelectron spectroscopy was used to check the purity of the Ga_2O_3. Peaks other than Pd, Ga, and O were absent in Pd/Ga_2O_3, thus potential contaminants are below the detection limit. After impregnation the catalysts were dried at 373 K for 48 h and subsequently calcined at 773 K for 4 h in static air. The Pd particle size of the reduced catalyst determined from transmission electron microscopy (TEM) micrographs is 2.9 ± 0.7 nm. All reductive pretreatments were performed in situ directly before FTIR measurements.

2.2. Temperature-Programmed Surface Reaction. Temperature-programmed surface reaction was followed by FTIR using a Bruker Vertex 70 spectrometer (liquid N_2-cooled MCT detector, resolution of 4 cm^{-1}) and a high-vacuum transmission cell with a base pressure of 10^{-6} mbar. Samples were pressed into self-supporting wafers and placed in a small, cylindrical stainless steel sample holder equipped with a ring-shaped furnace and a type-K thermocouple mounted to the sample holder. The following pretreatment sequence was carefully chosen to reproducibly produce metallic or intermetallic particle surfaces for spectroscopic studies. All samples were subjected to an in situ oxidative pretreatment at 673 K in 100 mbar O_2 for 60 min, followed by another 30 min in vacuum before cooling to 323 K. Then, one of two different reductive treatments was performed in situ in 100 mbar H_2 and 800 mbar N_2. For low temperature reduction (LTR) the sample temperature was raised to 373 K, for high-temperature reduction (HTR) to 673 K, where the sample was kept for 60 min, followed by another 30 min in vacuum at the respective reduction temperature. The LTR sample was then subjected to an additional heating step in vacuum to 673 K to ensure a reproducibly clean surface. Subsequently, a blank heating ramp from 323 to 673 K in high vacuum was run to record background spectra of the clean, reduced sample at each temperature to be subtracted from the spectra recorded during TPSR-IR. Methanol (Sigma Aldrich, p.a. ≥99.8%) was kept water-free by storing it over molecular sieve and was degassed by performing repeated freeze−pump−thaw cycles immediately prior to the introduction into the measurement cell. After adsorption at 323 K and 0.1 mbar for 10 min the cell was evacuated for another 10 min before starting a heating ramp (5 K/min) to 673 K, where the sample was kept for another 30 min. Spectra were recorded every minute throughout the experiment.

2.3. Steady State in Situ FTIR. Steady state in situ FTIR measurements were performed on a Bruker IFS 28 spectrometer (liquid N_2-cooled MCT detector, resolution of 4 cm^{-1}) with a stainless steel absorption flow cell of similar construction to the cell described in section 2.2. Instead of a vacuum system, the cell is connected to a gas manifold system with calibrated mass flow controllers. The sample was pretreated by reduction in 25% H_2/N_2 at 673 K for 60 min, flushing in N_2 for another 30 min and cooling to reaction temperature. All spectra shown were recorded at 498 K, with a time resolution of about 1 spectrum every 120 s. The reactants CH_3OH and H_2O were introduced by passing two separate He flows through temperated saturators, resulting in a molar ratio of 1:1 at a total flow of 40 mL/min in MSR (1 vol % CH_3OH/1 vol % H_2O/He). In methanol decomposition (MDC), all flows were the same, only the H_2O-containing saturator was passed by (1 vol % CH_3OH/He).

2.4. Concentration Modulation FTIR Spectroscopy. Diffuse reflectance infrared Fourier transform spectroscopy (DRIFTS) data were acquired using a Bruker Vertex 70 spectrometer (liquid N_2-cooled MCT detector, 4 cm^{-1} resolution). A home-built spectroscopy cell, adapted from the Harrick HVC-DRP cell but with a smaller dead volume was attached to a gas manifold system with calibrated mass flow controllers. In this geometry, the reactant flow passes from the top through the catalyst bed. Solenoid valves, electronically triggered using the rapid scan option of the OPUS software (Bruker Optics), were placed directly in front of the cell to further minimize dead volume and allow for a rapid switching between reactant flows. Analysis of the product gas flow was performed online using a mass spectrometer (Pfeiffer

Omnistar). Pretreatment was performed in situ in 25 vol % O_2/Ar at 723 K and subsequent reduction in 25 vol % H_2/Ar at 673 K. In concentration modulation measurements, the sample was contacted alternately with a flow of 1 vol % CH_3OH/1 vol % H_2O/Ar and 1 vol % CH_3OH/Ar at a constant total flow of 40 mL/min. Experiments were performed using three period lengths of 51, 82, and 162 s over a total of 60, 30, or 20 modulation periods, respectively. During one modulation period, 60 (120 in the case of the longest period) consecutive and equally long time-resolved spectra were collected. Time resolved spectra were averaged over all modulation periods, excluding the first 5 periods the system takes to reach the quasi steady state around which it subsequently oscillates. The averaged time-resolved spectra were then processed mathematically into phase resolved spectra using phase-sensitive detection (PSD).[25,26]

3. RESULTS AND DISCUSSION

3.1. Temperature-Programmed Surface Reaction (TPSR-IR). Formation of the supported intermetallic compound Pd_2Ga by high temperature reduction of Pd/Ga_2O_3 catalysts leads to strongly enhanced catalytic properties in methanol steam reforming (MSR) compared to the low-temperature reduced, metallic Pd-containing catalyst.[8−10] To identify differences in the evolution of surface-adsorbed species over Pd_2Ga/Ga_2O_3 vs Pd/Ga_2O_3 that cause these different catalytic properties, the adsorption and conversion of methanol on both systems was compared by temperature programmed surface reaction monitored by FTIR spectroscopy (TPSR-IR). To single out the effect of intermetallic formation on the ability to adsorb and convert methanol, the effect of high-temperature reduction on the adsorption properties of the pure Ga_2O_3 support was studied in section 3.1.1 before turning to the Pd containing catalyst in sections 3.1.2 and 3.1.3.

3.1.1. β-Ga_2O_3 Support. According to the procedure described in section 2.2, β-Ga_2O_3 was prereduced at either 373 K or 673 K, the reduction temperatures used to produce metallic and intermetallic particles, respectively, on the supported catalyst. High-temperature reduction of Ga_2O_3 can result in the formation of Ga−H bonds and oxygen vacancies on the surface.[27] To assess the influence of such treatments on the interaction of β-Ga_2O_3 with methanol, TPSR-IR was performed in an analogous manner after both reduction treatments.

Figure 1 shows spectra recorded during heating the CH_3OH-exposed, 373 K reduced sample in vacuum between 373 and 673 K. It turned out that the observed species, as well as their evolution with increasing temperature proved to be identical on the 673 K reduced sample. Therefore, only the final spectrum at 673 K is shown in Figure 1 and the following discussion applies to TPSR-IR spectra recorded after both pretreatments. The whole set of spectra obtained during TPSR after reduction of Ga_2O_3 at 673 K can be found in the Supporting Information.

Chemisorbed methoxy (CH_3O) species are detected on the surface of Ga_2O_3 upon adsorption of CH_3OH at 323 K, evacuation and heating to 373 K. They are characterized by the ν(C−O) band at 1065 cm^{-1}. That is in agreement with the values of 1095 cm^{-1} observed for Al_2O_3,[28] 1055 cm^{-1} for ZnO[29] and 1070 cm^{-1} for Ga_2O_3.[30] Corresponding $\rho(CH_3)$ and $\delta(CH_3)$ bands are observed at 1185 cm^{-1} and around 1475 cm^{-1}, respectively.[31] Simultaneously, several negative OH bands appear in the region 3800−3500 cm^{-1}, due to isolated OH on the surface being shifted to lower wavenumbers by an

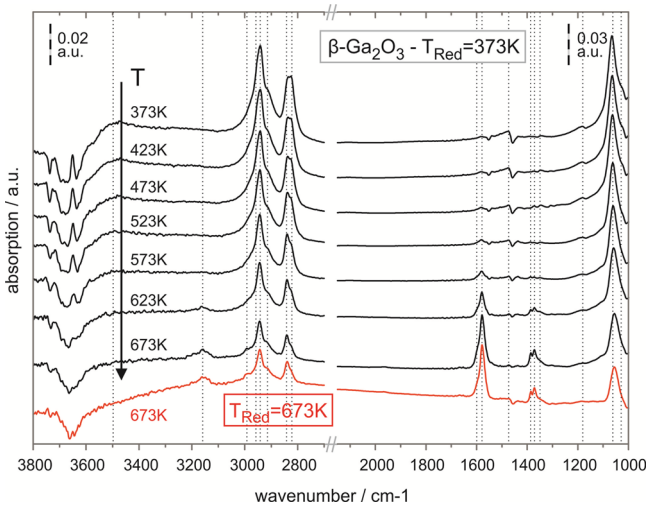

Figure 1. FTIR spectra of β-Ga_2O_3 reduced at 373 K, recorded after adsorption of CH_3OH, during heating from 373 to 673 K in high vacuum. Bottom spectrum (red, color online) recorded on 673 K-reduced sample.

H-bonding interaction with adsorbed CH_3O.[32] Physisorbed CH_3OH is likely present in small amounts, evidenced by a ν(C−O) shoulder at 1030 cm^{-1} and a broad ν(O−H) band around 3500 cm^{-1}. In the 2800−3000 cm^{-1} wavenumber region, bands were observed at 2825, 2840, and 2940 cm^{-1}, with shoulders at around 2915 and 2950 cm^{-1}. The assignment of signals in this region is not unambiguous. Bands to be expected in this wavenumber regime include $\nu_{sym}(CH_3)$, $\nu_{asym}(CH_3)$, the overtones $2\delta_{sym}(CH_3)$ and $2\delta_{asym}(CH_3)$, all potentially originating from various adsorbed species (at least CH_3OH, CH_3O and formates). According to a recent interpretation scheme by Collins et al. on Ga_2O_3,[30] bands at 2825 and 2940 cm^{-1} are assigned to ν_{sym} and $2\delta_{asym}$ of CH_3O, while the bands at slightly higher wavenumber (2840 and 2950 cm^{-1}) are assigned to ν_{asym} and $2\delta_{asym}$ of physisorbed CH_3OH. Busca et al. have assigned a band around 2830 cm^{-1} to $2\delta_{sym}(CH_3)$ and a pair of bands in the 2950 cm^{-1} region to symmetric and asymmetric $\nu(CH_3)$ of adsorbed methoxy, respectively.[33] Bands at 2817 and 2932 cm^{-1} on the closely related ZnO system have been assigned to $\nu_{sym}(CH_3)$ and $\nu_{asym}(CH_3)$ of CH_3O, respectively.[29] A similar assignment was performed by Bertarione et al. on MgO.[34] During the temperature-programmed experiment, bands at 1030 and 3500 cm^{-1}, assigned to ν(C−O) and ν(O−H) of physisorbed CH_3OH disappear, while the bands at 2825 and 2840 cm^{-1} both remain up to 673 K. Therefore, the assignment of the latter band to physisorbed CH_3OH, as proposed in the literature,[30] is unlikely. Instead, the observation of at least 5 bands stable in vacuum at up to 673 K in this region indicates the presence of more than one type of CH_3O species, adsorbed to different Ga_2O_3 sites. Ga_2O_3 exposes tetrahedrally and octahedrally coordinated Ga sites on its low-index surfaces.[35] A further possibility is the presence of a more strongly bound type of associatively adsorbed methanol, as was reported previously for Al_2O_3.[28,32]

Judging from the ν(C−O) intensity (1065 cm^{-1}), adsorbed CH_3O shows remarkable stability and remains at the surface of β-Ga_2O_3 in significant amounts up to 673 K. Starting from 573 K, coincidentally with a decrease in the ν(C−O) of methoxy, a new set of bands appears at 1580, 1386, and 1370 cm^{-1} with

dx.doi.org/10.1021/cs300480c | ACS Catal. 2012, 2, 2305−2315

shoulders at 1600 and 1350 cm^{-1}. These bands can be assigned to adsorbed formate (HCOO) species, produced from CH_3O by reaction with either lattice O of Ga_2O_3 or surface OH groups. According to a recent DFT study on the stability of formate species on Ga_2O_3,[36] the sharp bands at 1580, 1386, and 1370 cm^{-1} can be assigned to a bridging formate species (br-HCOO), while the band at 1600 cm^{-1} is assigned to a bidentate formate (β-HCOO). Corresponding ν(C−H), ν_{asym}(COO + δCH) combination, and $2\nu_{asym}$(COO) overtone bands assigned to br-HCOO are observed as well at 2917, 2994, and 3160 cm^{-1}, respectively. In addition to b-HCOO, a band due to monodentate formate (m-HCOO) is expected at the position of the band at 1350 cm^{-1}. The kinetic differentiation of various species (section 3.4) under reaction conditions was helpful with respect to further band assignment.

Our study of adsorbed species during conversion of CH_3OH on β-Ga_2O_3 is in general agreement with the literature.[30] Most importantly, we could show that the high temperature reductive treatment that induces intermetallic compound formation on the Pd/β-Ga_2O_3 catalyst has no observable effect on the adsorption and conversion of methanol on the pure β-Ga_2O_3 support. This corresponds well with previous in situ XPS studies, which showed no changes in the Ga 3d binding energy region of β-Ga_2O_3 upon high temperature reduction.[10]

3.1.2. Pd/Ga_2O_3 Catalyst (LTR). Figure 2 shows spectra recorded during TPSR-IR of adsorbed methanol between 373 and 673 K on Pd/β-Ga_2O_3 reduced at 373 K. This treatment produces metallic Pd particles supported on Ga_2O_3.[10]

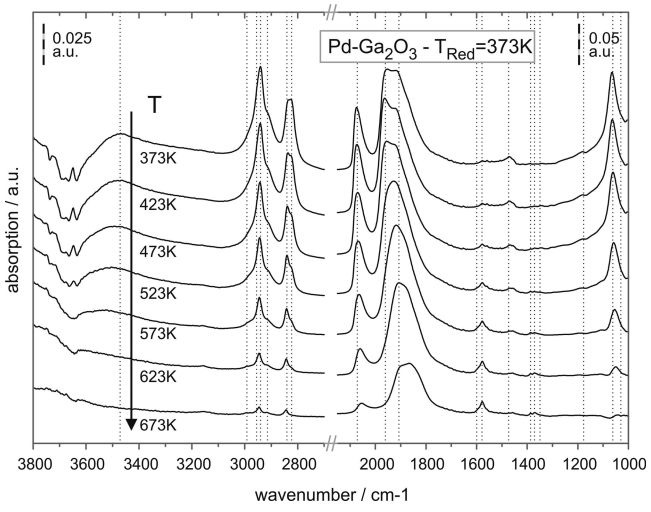

Figure 2. FTIR spectra of Pd/Ga_2O_3 reduced at 373 K, recorded after adsorption of CH_3OH, during heating from 373 to 673 K in high vacuum.

Similarly to the Ga_2O_3 support, mainly CH_3O species are present on the Ga_2O_3-support surface. They are characterized by a ν(C−O) feature at 1065 cm^{-1} as well as the r(CH_3) and δ(CH_3) modes at 1185 cm^{-1} and 1475 cm^{-1}, respectively. A weak shoulder around 1030 cm^{-1} and a broad band around 3500 cm^{-1} indicate the presence of small amounts of physisorbed CH_3OH. In the CH stretching region, bands are observed at 2825, 2840, and 2940 cm^{-1}, with shoulders around 2915 and 2950 cm^{-1}. In addition to the features of Ga_2O_3, the typical intense bands of adsorbed CO on particles of metallic Pd are observed, with a signal at 2075 cm^{-1} assigned to CO adsorbed linearly on metallic Pd atoms, one at 1955 cm^{-1} assigned to bridge bonded CO on edges/steps or (100) facets and one at 1915 cm^{-1} corresponding to hollow- or bridge bonded CO on (111) facets.[37] The presence of these bands shows that dehydrogenation of CH_3OH to CO takes place on the surface of metallic Pd particles[38,39] already at 373 K.

At the same time however, methoxy species are still present on the support surface. Intermediate species of methanol decomposition on metallic Pd, such as an additional CH_3O species, formyl (HCO) or formaldehyde (HCHO)[40,41] are not observed, indicating a rapid dehydrogenation of methanol on Pd. TPSR-IR clearly shows that, compared to pure Ga_2O_3, where CH_3O is still present at 673 K, these species react at lower temperatures in the presence of metallic Pd. Likely explanations are either (i) a migration of CH_3O species[42] to Pd at higher temperatures and subsequent dehydrogenation to CO or (ii) an acceleration of CH_3O dehydrogenation on Ga_2O_3 by Pd acting as a sink for the liberated atomic H. Oxidation of remaining CH_3O species to adsorbed HCOO takes place in a similar temperature range as on the pure Ga_2O_3 (≥573 K). The final intensity of bands at 1580, 1386, and 1370 cm^{-1} is smaller here, likely because the majority of CH_3O species has already reacted in the competing dehydrogenation pathway on Pd at lower temperatures.

3.1.3. Pd_2Ga/Ga_2O_3 Catalyst (HTR). Figure 3 shows spectra recorded during TPSR-IR of adsorbed methanol between 373 and 673 K after reduction of Pd/β-Ga_2O_3 at 673 K. Reduction at this temperature generates intermetallic Pd_2Ga particles supported on Ga_2O_3.[10] Similarly to the Ga_2O_3 support and the Pd/Ga_2O_3 sample, CH_3O species chemisorbed on Ga_2O_3 are detected. CO adsorbed to Pd atoms within the intermetallic compound Pd_2Ga is detected as well, characterized by a sharp, asymmetric, and very intense band at 2075 cm^{-1}. Two additional carbonyl bands at 1940 and 1885 cm^{-1} are assigned to CO adsorbed on domains of metallic Pd formed on the surface of the intermetallic Pd_2Ga particles under reaction conditions.[10,11]

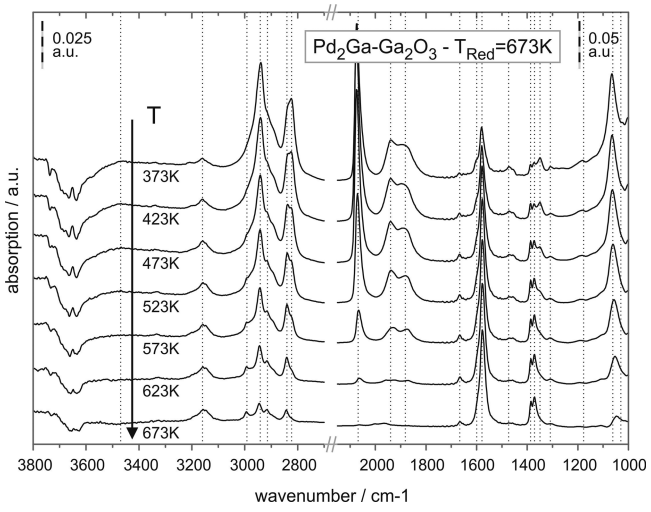

Figure 3. FTIR spectra of Pd_2Ga/Ga_2O_3 reduced at 673 K, recorded after adsorption of CH_3OH, during heating from 373 to 673 K in high vacuum.

The most pronounced difference to Ga_2O_3 and Pd/Ga_2O_3 is the presence of significant amounts of formates on Pd_2Ga/Ga_2O_3 already at 373 K. Bands are observed at 1580, 1386, and 1370 cm^{-1} (br-HCOO), at 1600 and 1350 cm^{-1} (b-HCOO),

dx.doi.org/10.1021/cs300480c | ACS Catal. 2012, 2, 2305−2315

and at 1660, 1350, and 1305 cm^{-1} (m-HCOO).[36] Generally, the intensity of formate-related bands increases coincidentally with a decrease of the amount of adsorbed methoxy species, corroborating the sequence $CH_3OH_{ads} \rightarrow CH_3O_{ads} \rightarrow HCOO_{ads}$. Compared to Pd/Ga_2O_3, methoxy species (ν(C–O) = 1030 cm^{-1}) are slightly more stable on Pd_2Ga/Ga_2O_3; small amounts are still detected at 673 K, indicating that the dehydrogenation pathway to CO, that prevails on metallic Pd is slower on the intermetallic particles (patches of metallic Pd are mainly responsible for remaining methoxy dehydrogenation to CO[10]). The question arises why the formation of formates from adsorbed methoxy is so strongly enhanced on Pd_2Ga/Ga_2O_3 compared to Pd/Ga_2O_3 and pure Ga_2O_3.

It should be kept in mind that the reaction of adsorbed CH_3O to HCOO requires a source of reactive oxygen, that is, lattice O or OH groups, and is enhanced by a sink for the atomic H liberated during the reaction.[24] The latter point can likely be fulfilled by both Pd and Pd_2Ga, as both are active hydrogenation catalysts.[43] Reactive oxygen species, however, may be formed on the Ga_2O_3 support by high temperature reduction in the presence of Pd and subsequent formation of intermetallic Pd_2Ga. Atomic H formed on Pd during prereduction can spill over and reduce Ga_2O_3 to more volatile Ga_2O.[44] This suboxide may diffuse to the Pd particle, proceed to form the intermetallic compound there, and leave behind a support surface containing the oxygen species that react easily with adsorbed CH_3O. The precise nature of this reactive oxygen species remaining on the atomic H-treated Ga_2O_3 support is presently not understood. In any case, the strongly facilitated oxidation of CH_3O to HCOO after high-temperature reduction and intermetallic formation indicates the presence of such a species. The involvement of lattice O in the formation of formates has been proposed by Akhter et al.[45] on ZnO, and was enhanced in the presence of Cu.[46] The direct involvement of OH groups in the oxidation of CH_3O to HCOO is not indicated by the experimental results, as the OH stretching region on Pd/Ga_2O_3 (no formates) and Pd_2Ga/Ga_2O_3 (high surface formate concentration) shows precisely the same features.

br-HCOO appears to be the most stable formate species, with its bands increasing in intensity up to 673 K. b-HCOO and m-HCOO are less stable, but are both still detected at 673 K. A strong decrease of the 1350 cm^{-1} band between 373 K and 523 K indicates that in addition to m-HCOO and b-HCOO there may be another species contributing at this wavenumber, since there is no correlated decrease in either the 1600 or the 1660 cm^{-1} band. Since the intensity decrease in this region is strong between 373 and 523 K, a temperature region where the surface concentration of all formate species increases and no CH_3O related band is expected there, we tentatively assign a band at this position to an intermediate in the transformation of methoxy into formate species. Formaldehyde adsorbed in η^2 geometry has been shown to produce bands in a similar wavenumber region (1255 and 1305 cm^{-1} according to ref 40).

In summary, TPSR-IR on Pd/Ga_2O_3 and Pd_2Ga/Ga_2O_3 revealed pronounced differences in the temperature-dependent evolution of surface adsorbed species. While Pd/Ga_2O_3 behaves similar to pure Ga_2O_3 with respect to the formation of surface formates from methoxy, formate species are formed at much lower temperatures on the high-temperature reduced intermetallic Pd_2Ga/Ga_2O_3 sample. We propose that formate formation is facilitated by the presence of certain sites on Ga_2O_3, which are formed during high-temperature reduction and intermetallic compound formation and supply the reactive oxygen needed to oxidize adsorbed CH_3O to HCOO.

3.2. Steady State in Situ FTIR. While TPSR-IR in high vacuum yielded interesting conclusions on the varying extent of formate formation on Pd_2Ga/Ga_2O_3 vs Pd/Ga_2O_3 and Ga_2O_3, steady state flow in situ FTIR experiments are necessary to study adsorbed surface species under actual reaction conditions of methanol decomposition (MDC) (i.e., dehydrogenation) and steam reforming (MSR). Pretreatment was performed by reducing the catalyst at 673 K (HTR) that produces Pd_2Ga/Ga_2O_3.[10] Investigation of the catalytic properties of a sample prepared in this manner showed that H_2 and CO_2 are the main products during MSR,[10] while methyl formate and CO are mainly produced alongside H_2 in MDC.[8]

Spectra recorded in situ during methanol dehydrogenation and methanol steam reforming at 498 K are presented in Figure 4 (solid black lines). In general, in situ FTIR corroborates the

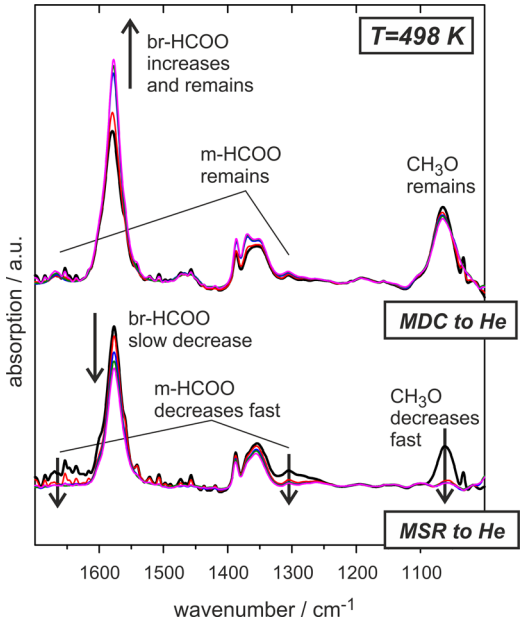

Figure 4. In situ FTIR spectra recorded at 498 K under MDC and MSR reaction conditions (black solid lines) and every 2 min after switching from reaction mixture to a pure He flow (red-blue-green-magenta, color online).

results gained from vacuum TPSR-IR. Identical surface species are observed. Most importantly, the presence of large amounts of formates (main signal at 1580 cm^{-1}) on Pd_2Ga/Ga_2O_3 is confirmed under reaction conditions. An additional experiment, in which both reactions were performed on a low-temperature reduced (i.e., metallic, LTR) Pd/Ga_2O_3 sample, showed much smaller amounts of formates, again in agreement with TPSR-IR (spectra not shown for the sake of brevity). Interestingly, the presence of H_2O, which has been shown to drastically alter catalytic properties[10] does not lead to the detection of new surface species. It is, however, apparent from comparing the two sets of spectra in Figure 4 that CH_3O and HCOO signals are clearly more intense in the absence of H_2O. This does imply a role of H_2O on the reactivity and stability of carbonaceous surface species. After 30 min of reaction at 498 K, the reactant flow was changed from MDC/MSR conditions to He at 498 K (see Figure 4). The response of adsorbed CH_3O and HCOO

dx.doi.org/10.1021/cs300480c | ACS Catal. 2012, 2, 2305–2315

species greatly differs between the two cases. When switching from MDC (i.e., only CH_3OH/He is fed) to He, CH_3O species remain unperturbed (cfr. intensity of the 1065 cm^{-1} signal corresponding to ν(C-O)). At the same time, signals corresponding to b- and br-HCOO increase after switching to He and then remain unaffected even when flushing in He for 30 min. The 1660 and 1305 cm^{-1} signals corresponding to m-HCOO are stable as well. On the other hand, when switching from MSR (i.e., CH_3OH/H_2O/He) to He, the 1065 cm^{-1} methoxy signal disappears almost instantly, as it would be expected from a reaction intermediate. The same applies to m-HCOO but not to br-HCOO, which shows a much slower decrease of its characteristic band at 1580 cm^{-1}. Some formate species, however, are so stable that they are still present in significant amounts after long exposure to He (spectra not shown) thus ruling out their role as reaction intermediates.

In summary, in situ FTIR experiments enabled us to confirm the identity of species present during the reactions of MDC and MSR. Results strongly support and complement those obtained from vacuum TPSR-IR. Most importantly we could show that the presence of H_2O plays an important role in determining the reactivity of surface species on Pd_2Ga/Ga_2O_3. When H_2O is present, the entire system behaves more dynamically. The concentration of adsorbed species (CH_3O and HCOO) is smaller, presumably because of faster surface reactions. In the absence of H_2O, however, CH_3O and HCOO species appear to be strongly adsorbed at the surface and hardly show any response to a change in the reactant concentration.

3.3. Concentration Modulation FTIR Spectroscopy. To clarify the role of H_2O as a reactant in the conversion of methanol over Pd_2Ga/Ga_2O_3, in situ concentration modulation spectroscopy was applied. The concentration of H_2O in the feed was modulated between 0 and 1 vol % over a total of 30 modulation periods of 82 s each. Prior to the modulation sequence, the catalyst was equilibrated with an equimolar feed of CH_3OH and H_2O. Surface adsorbed species were continuously monitored by DRIFTS, and reaction products were simultaneously analyzed by MS.

Figure 5 presents selected MS traces recorded over 3 consecutive modulation periods. The system continuously and reversibly alternated between two reactivity states; one in the presence of H_2O with H_2 and CO_2 as main products (i.e., MSR) and the other without H_2O, with H_2, CO, and MFO as main products (i.e., MDC) at lower overall conversion of CH_3OH. At the end of each 41 s half-period, a steady reaction state was reached, and the catalytic properties were stable over all modulation periods. The most striking feature of the MS traces is the presence of pronounced spikes of MFO (m/z = 60), CH_3OH (m/z = 31), and CO (m/z = 28) at the $CH_3OH \rightarrow H_2O + CH_3OH$ switch. Apparently, at the very moment H_2O is admitted the production of these species is transiently enhanced before a lower steady state level is attained in the H_2O pulse. Notably, the mass trace of H_2 (m/z = 2) does not show a corresponding spike. Therefore, we conclude that the following reaction occurs immediately after reintroducing H_2O into the reaction system.

$$HCOOCH_3 \rightarrow CH_3OH + CO \quad (2)$$

The decomposition of MFO to CH_3OH and CO over a number of catalysts has been described in the literature. Jiang et al.[19] showed it occurs to a small extent over Cu catalysts during MSR. A MSR mechanism was proposed in which intermediate MFO is hydrolyzed to formic acid and further reacts to the

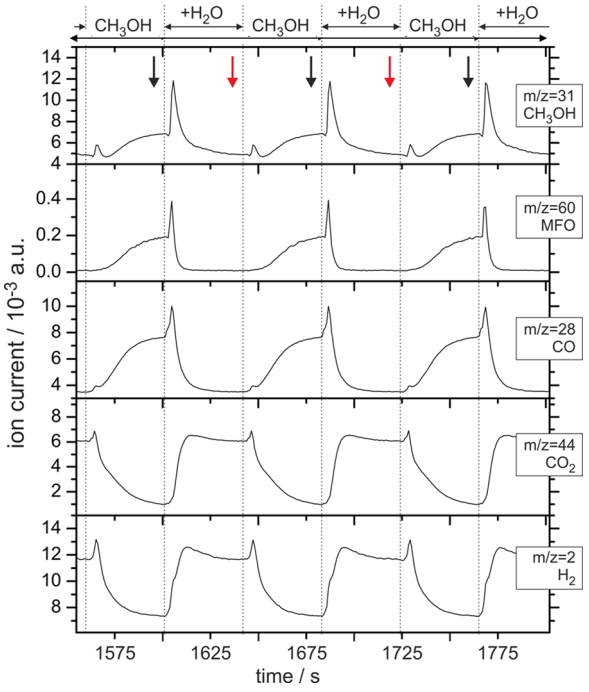

Figure 5. Selected MS traces recorded during three consecutive $CH_3OH/CH_3OH + H_2O$ modulation periods. Arrows indicate when the spectra used to calculate the averaged spectra shown in Figure 7 (top) were recorded.

products H_2 and CO_2. Decomposition of MFO was proposed to be responsible for CO byproduct formation on these systems.

The interpretation that MFO decomposition occurs during the transition from MDC to MSR is supported by another experiment at 573 K showing the same spikes in the mass spectra (not shown). However, MFO was produced to a much lesser extent, while more CO and CH_3OH were produced, indicating that the MFO decomposition reaction is almost complete at the higher reaction temperature. An important conclusion from the observed, facile decomposition of MFO to CO and CH_3OH over Pd_2Ga/Ga_2O_3 is that MFO is not likely to be an intermediate in the selective MSR reaction on this system. MFO has been proposed as an intermediate in MSR on Cu-based catalysts[19,47] but has been considered irrelevant in recent theoretical studies.[22] The question arises on the origin of MFO during the switch from H_2O-free to H_2O-containing conditions. Either MFO accumulates on the surface during the H_2O-free pulse and is then desorbed in the presence of H_2O or another adsorbed species is converted to MFO rapidly upon introduction of H_2O. To possibly identify such species, the DRIFTS data recorded during the concentration modulation experiment should be helpful.

Figure 6 shows the kinetics of selected FTIR signals over the same three modulation periods of Figure 5. The depicted signals are the ν_{asym}(COO) of m-HCOO at 1660 cm^{-1}, the ν_{asym}(COO) of b-/br-HCOO (unresolved in time-resolved spectra) at 1580 cm^{-1}, and the δ(C−H) mode of CH_3O at 1460 cm^{-1}. Surface species appear to accumulate during the H_2O-free pulse and react faster in the presence of H_2O, thus confirming the tendency observed in section 3.2. Competitive adsorption between H_2O and CH_3OH and/or HCOO may contribute to this effect. However, the pronounced changes in the product distribution observed by MS indicate that the

dx.doi.org/10.1021/cs300480c | ACS Catal. 2012, 2, 2305−2315

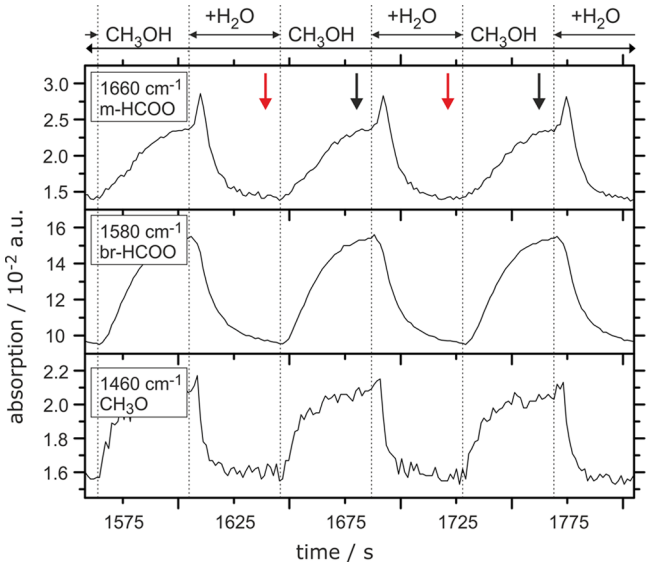

Figure 6. Selected FTIR traces recorded during three consecutive CH_3OH/CH_3OH+H_2O modulation periods. Arrows indicate when the spectra used to calculate the averaged spectra shown in Figure 7 (top) were recorded.

reaction sequence is fundamentally altered in the presence of H_2O. It is obvious that the m-HCOO signal at 1660 cm^{-1} correlates very closely with the spikes observed in the MS data (Figure 5). Simultaneously to the production of MFO, CO, and CH_3OH, the surface concentration of m-HCOO increases sharply. This m-HCOO may be formed from b-/br-HCOO, as the temporal evolution of the (unresolved) 1580 cm^{-1} signal is characterized by a decrease in intensity from the moment H_2O is switched on. A change of adsorption geometry from bridging/bidentate to monodentate by the coadsorption of H_2O has previously been proposed on the related ZnO system.[48] After its H_2O-assisted formation, m-HCOO reacts with CH_3O species accumulated on the catalyst in the absence of H_2O, to produce MFO (detected by MS). Once the supply of surface CH_3O is reduced (see sharp drop of δ(C−H) intensity in Figure 6), the reaction proceeds with OH, formed by H_2O adsorption, instead of CH_3O and in the direction of selective MSR. Judging from the lower intensity of the m-HCOO signal under steady state MSR conditions, the reaction with OH appears to be faster than the reaction with CH_3O resulting in a smaller surface concentration of the m-HCOO intermediate. In a last step, H_2 and CO_2 are formed, likely over a formic acid intermediate, which could, however, not be detected by FTIR in this study.

At 573 K (spectra not shown) the signal of m-HCOO is generally smaller than at 523 K. Since higher temperatures should rather benefit monodentate adsorption geometry (T-pulses have been used to deliberately transform br-HCOO into m-HCOO[49]), this further indicates the reactive nature of the m-HCOO intermediate, which reacts faster at 573 K resulting in a smaller surface concentration detected by FTIR.

3.4. Phase Sensitive Detection (PSD). To gain more information on the correlation of FTIR signals and on their kinetic response, the same set of spectral data was treated with PSD.[25,26] The main advantage of PSD is its selectivity in the detection of species responding to a certain external stimulation. By choosing a suitable stimulation, in our case a modulation of the H_2O concentration in the reactant feed, it is possible to distinguish between adsorbed spectator species that do not show any response to the modulation and species that show a periodic response and therefore are more likely involved in the catalytic cycle. Furthermore, surface species can be distinguished by the phase delay between the excitation and their spectral response, with the additional advantage of a generally increased signal-to-noise ratio, because of the averaging over a number of modulation periods.

Figure 7 presents two selected averaged time-resolved spectra recorded at the end of each half period and the

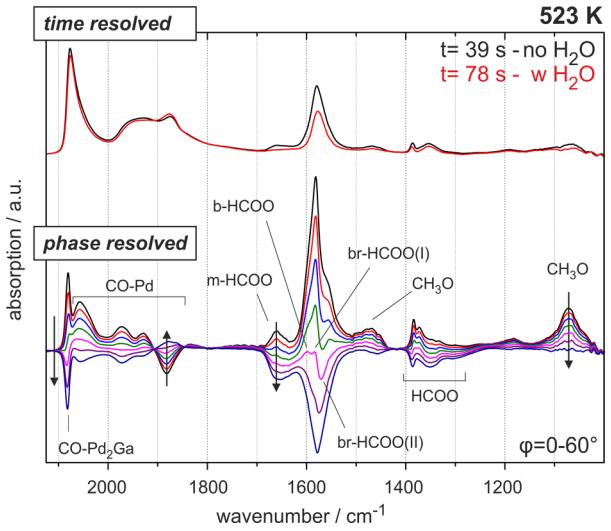

Figure 7. Selected averaged time-resolved spectra recorded at the end of each half-period (top) and corresponding phase-resolved spectra in a phase angle range of 0−60° calculated using PSD.

corresponding phase resolved spectra in the phase angle range of 0−60°. Comparison of time- and phase resolved spectra shows that while carbonyls show the strongest signals in the time-resolved spectra, formates are much more intense in the phase resolved ones. Also CH_3O species appear strongly enhanced in the phase-resolved spectra. This demonstrates that the latter species show a stronger response to the modulation of H_2O concentration.

Additionally, PSD spectra present the possibility of resolving complex signals that cannot be resolved in time-resolved spectra. Large and static signals do not appear in phase resolved spectra. Moreover, signals and therefore species showing a different kinetic response exhibit their maximum/minimum intensity at different phase angles. The phase angle at which a signal disappears in phase resolved spectra is referred to as its out-of phase angle Φ_{out}, whereas the phase angle of maximum intensity is the in-phase angle Φ_{in}. In Figure 7, the enhanced spectral resolution provided by PSD can be clearly observed in the carbonyl region. While time-resolved spectra showed only one asymmetric carbonyl band at 2078 cm^{-1}, and 2 broader signals at 1940 and 1880 cm^{-1}, PSD enables us to differentiate between a very narrow signal at 2080 cm^{-1} and a broader one at 2058 cm^{-1}. Furthermore, the broad band at 1940 cm^{-1} is shown to consist of 2 contributions at 1970 and 1930 cm^{-1}. Because of the pronounced difference in bandwidth we assign the sharp, high energy feature to CO adsorbed linearly on Pd atoms of the intermetallic Pd_2Ga particles. Such a CO species has been proposed in the literature to show no coverage dependent frequency shift,[50] which explains the very narrow nature of the band. The broader lower energy features are

dx.doi.org/10.1021/cs300480c | ACS Catal. 2012, 2, 2305−2315

Table 1. IR Frequencies of Adsorbed Formate Species, ν(COO) Frequency Split $\Delta\nu = \nu_{asym} - \nu_{sym}$, and out-of-Phase Angles Φ_{out} in PSD Determined According to Reference 26

	br-HCOO (I)		b-HCOO		br-HCOO (II)		m-HCOO	
	$\tilde{\nu}$/cm^{-1}	Φ_{out}	$\tilde{\nu}$/cm^{-1}	Φ_{out}	$\tilde{\nu}$/cm^{-1}	Φ_{out}	$\tilde{\nu}$/cm^{-1}	Φ_{out}
ν_{asym} COO	1580	201°	1600	200°	1570	187°	1660	174°
ν_{sym} COO	1370	210°	n.d.[a]		1330	185°	1305	174°
δ CH	1386	207°	n.d.		1360	190°	1350	173°
$\Delta\nu$	210		n.d.		240		355	

[a]"n.d." means "not detected".

assigned to CO adsorbed to different sites on domains of metallic Pd.[37] Looking at the phase angle dependence of the carbonyl signals, one notices that the signal at 1880 cm^{-1}, assigned to adsorbed CO on hollow Pd sites, shows an opposite behavior to all other carbonyl signals. It is the only signal with increased intensity in the presence of H_2O. The explanation for this behavior of hollow bonded CO is unclear. It may be simply due to a shift in the preferred adsorption geometry in the presence of H_2O, which may be caused by the lower CO partial pressure during MSR than during MDC (see Figure 5). However, because of its peculiar phase dependent behavior, and its increased intensity under selective steam reforming conditions, one may argue it can be involved in a pathway of MSR or in one of its side reactions. Clearly further studies are needed to clarify this point.

In the frequency range of formate-related bands, a wealth of new information can be extracted from phase sensitive spectra. While m-HCOO was very weak and b- and br-HCOO could not be resolved in time-resolved spectra, the situation is much improved in PSD. A pronounced signal due to m-HCOO is observed at 1660 cm^{-1}, and an additional weak broad signal related to adsorbed H_2O can be discerned around 1630 cm^{-1}. The signal at 1600 cm^{-1} due to b-HCOO can now be resolved from the larger one at 1580 cm^{-1} due to br-HCOO, although the kinetic response of these species is very similar. A new signal is clearly observed at about 1570 cm^{-1}. It exhibits a different kinetic behavior than the signals at 1580 and 1600 cm^{-1}, which is the very reason it can be detected in PSD, in spite of the strong, neighboring signal at 1580 cm^{-1}. An unambiguous assignment of this signal is difficult because it was not considered in previous FTIR studies and theoretical calculations. Formate species are generally identified in IR spectroscopy according to the split between their ν_{sym}(COO) and ν_{asym}(COO) signals.[51] We have attempted to analyze the ν_{sym}(COO) and δ(C−H) frequency region (1300−1400 cm^{-1}) by analyzing the kinetic response of selected signals (more specifically their out-of-phase angles Φ_{out}, that is, the phase angle at which the IR signal of a species vanishes[26]) and comparing them with the responses of the larger, more easily assigned ν_{asym}(COO) bands. It should be noted that for the determination of out-of-phase angles, the experiment at shorter modulation periods (51 s) was chosen, as small differences in kinetics were more easily observed than in the longer modulation periods. The results of this comparison are shown in Table 1.

From a kinetic point of view, the assignment of signals at 1660, 1305, and 1350 cm^{-1} to m-HCOO is strongly corroborated, since all three signals show precisely the same phase delay. The assignment of signals at 1580, 1370, and 1386 cm^{-1} to br-HCOO is also supported by our data. The signals show very similar phase delay. No signals corresponding to the 1600 cm^{-1} ν_{asym}(COO) of b-HCOO could be identified. Two very small signals at 1330 and 1360 cm^{-1} may be the corresponding δ(C−H) and ν_{sym}(COO) modes of the new 1570 cm^{-1} formate signal. Their kinetic response is identical to that of the 1570 cm^{-1} signal. According to the frequency split of 240 cm^{-1}, we propose the signal at 1570 cm^{-1} can be assigned to an additional formate species in bridging geometry (br-HCOO (II)), which is adsorbed to Ga atoms of different coordination. It is well-known that low index surfaces of β-Ga_2O_3 contain tetrahedrally and octahedrally coordinated cations, Ga(t) and Ga(o), respectively, in a ratio of about 1:1.[35] The IR absorption frequency of adsorbed OH groups has been shown to differ, according to the coordination of the cation they are adsorbed to,[52] and the bond strength to adsorbed H differs by 24%, according to quantum chemical calculations.[53] Accordingly, an effect on the ν(COO) of adsorbed formates and a difference in reactivity is to be expected. If the signal at 1580 cm^{-1} is assigned to br-HCOO coordinated to two Ga(o) sites, and the signal at 1570 cm^{-1} to br-HCOO coordinated to a Ga(o)-Ga(t) site pair, the only "missing" species would be a Ga(t)-Ga(t) bridging one. However, in contrast to the former two, such a species could not be detected, in agreement with a study dealing with bridging OH groups, which also detected only Ga(o)-Ga(o) and Ga(o)-Ga(t) bridging groups on β-Ga_2O_3. Since in contrast to Ga(o) sites, surface Ga(t) atoms are coordinatively saturated, their adsorption strength may be weaker, explaining the apparent absence of bridging Ga(t)-Ga(t) species, but also the detection of only one m-HCOO and β-HCOO species.

The out-of-phase angles Φ_{out} in Table 1 can be used not only to confirm signal assignments, but also to compare different adsorbed species with respect to the phase shift of their spectral response relative to the excitation. m-HCOO shows the smallest phase shift of about 174° an indication that it is the species that most directly reacts to the modulation of H_2O concentration. The newly identified br-HCOO(II) species shows the second fastest response (phase shift of about 188°) and br-HCOO(I) and b-HCOO show the slowest, at a phase shift of about 205°. This is in general agreement with our conclusions from time-resolved spectroscopy that m-HCOO is immediately formed upon introduction of H_2O. Most likely it is formed from all bidentate and bridging species. However, the formate characterized by the signal at 1570 cm^{-1} appears more reactive than the ones characterized by signals at 1580 and 1600 cm^{-1}.

3.5. Proposed Reaction Mechanism. A comparison between well characterized Pd/Ga_2O_3 and Pd_2Ga/Ga_2O_3 catalysts, regarding adsorption and temperature programmed reaction of CH_3OH demonstrated strongly enhanced formation of adsorbed formates at low temperatures on Pd_2Ga/Ga_2O_3. We ascribe the facilitated formation of these species to the presence of reactive oxygen sites in the Ga_2O_3 surface, which are formed during high-temperature reduction and formation of

dx.doi.org/10.1021/cs300480c | ACS Catal. 2012, 2, 2305−2315

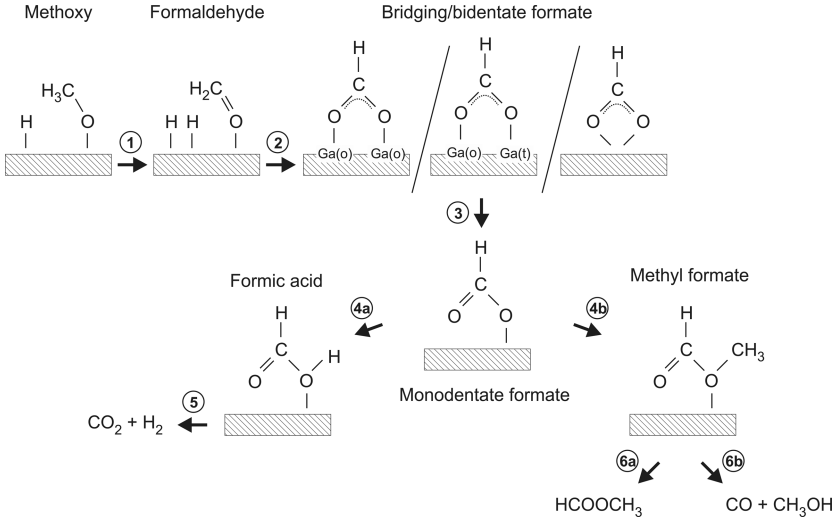

Figure 8. Schematic representation of mechanistic findings from vacuum- and in situ concentration modulation FTIR.

the intermetallic compound Pd_2Ga. Clearly, the reduction at 673 K in the presence of Pd leads to strong changes in the surface chemistry. In contrast, on Pd/Ga_2O_3 reduced at 373 K the absence of the reactive oxygen species and the fast dehydrogenation of methanol to CO and H_2 occurring on the metallic Pd surface are responsible for the absence of steam reforming activity with nearly 100% selectivity to CO and H_2 formation by methanol decomposition.[10]

The enhanced formate formation on the Pd_2Ga/Ga_2O_3 after reduction at 673 K observed in vacuum TPSR-IR was confirmed by in situ FTIR studies under reaction conditions. The stability of formate species in vacuum is very high, untypical for species involved in a catalytic reaction mechanism. This high stability is also found under reaction conditions of methanol decomposition (i.e., in the absence of H_2O). In the presence of H_2O, however, the entire adsorption system behaves more dynamically. Formates, and the methoxy species from which they are formed, react faster during methanol steam reforming (with H_2O as a reactant). The role of H_2O was studied in more detail by in situ concentration modulation FTIR spectroscopy, by periodically varying the concentration of H_2O while continuously collecting the spectral and catalytic response of the system. Clearly, this technique strongly complements vacuum and steady state in situ FTIR studies, by providing enhanced spectral and kinetic resolution of species. By correlating reactivity with surface species detected by FTIR, we could show that the transiently enhanced formation of methyl formate (MFO), CO, and CH_3OH is associated with a higher surface concentration of monodentate formate. We propose a mechanism (Figure 8) where H_2O converts stable bridging- and bidentate formates (formed from methoxy, likely over formaldehyde, (1) and (2)) into more reactive, monodentate species (3). These react either with adsorbed methoxy to methyl formate (4b) or with OH groups supplied by H_2O to CO_2 and H_2 (likely over intermediate formic acid (4a) and (5)). The reaction with OH is faster, leading to a smaller concentration of intermediate m-HCOO under MSR (i.e., H_2O-containing) conditions. In this mechanism, MFO is unlikely to be an intermediate in the selective MSR reaction to CO_2 and H_2. PSD in concentration modulation FTIR generally showed a strong response of formate and methoxy species on Ga_2O_3 to the modulated H_2O concentration. While carbonyls show the strongest absorption bands in time-resolved spectra, they are less pronounced in PSD spectra, indicating their minor role in the reaction compared to methoxy and formates. The presence of an additional formate species, characterized by a band at 1570 cm^{-1}, which cannot be resolved from the main br-HCOO species in time-resolved studies, can be discerned in PSD, due to the different kinetic behavior of the two formate species. The new formate species exhibited a slightly faster response to the concentration modulation. We therefore assign this species to a formate adsorbed in bridging geometry over a Ga(o)-Ga(t) site, while the slightly less reactive main species bridges two more coordinatively unsaturated Ga(o) sites. The Ga(o)-Ga(t) site may coincide with the reactive oxygen sites on the Ga_2O_3 surface that are produced upon formation of the intermetallic compound Pd_2Ga. To close the catalytic cycle the Ga_2O_3 surface has to be reoxidized by water. In a recent work of some of us[27] it was demonstrated that water can effectively reoxidize a reduced Ga_2O_3 surface even at room temperature. H_2 evolution was detected upon water dosing to Ga_2O_3 containing oxygen vacancies/defects and Ga−H formed by reduction. Reduction of the Ga_2O_3 by hydrogen and reoxidation by water appeared to be reversible processes.[27]

Finally, in agreement with a very recent in situ XPS study on PdGa (1:1) model surfaces,[12] this study emphasizes the role of the Ga_2O_3 support in the steam reforming of methanol. It can be deduced from our data that the reaction predominantly proceeds on the Ga_2O_3 surface modified by the high temperature reduction and intermetallic formation.

4. CONCLUSIONS

By utilizing FTIR spectroscopy to follow the interaction of methanol and water with Ga_2O_3, Pd/Ga_2O_3, and Pd_2Ga/Ga_2O_3 catalysts in situ, new insights into the reaction mechanism in MSR have been obtained. Strongly enhanced formation of surface formates with methanol at much lower temperatures was detected on Pd_2Ga/Ga_2O_3 compared to Ga_2O_3 and Pd/Ga_2O_3, which was assigned to the presence of reactive oxygen sites in the Ga_2O_3 formed during high-temperature reduction and formation of the intermetallic compound Pd_2Ga.

The dynamics and stability of methoxy and various formates was strongly dependent on the presence of water; these species react faster during methanol steam reforming than in a feed of

dx.doi.org/10.1021/cs300480c | ACS Catal. 2012, 2, 2305−2315

methanol only. Periodic variation of the concentration of H_2O in the feed with determination of the spectral and catalytic response of the system by FTIR spectroscopy and MS allowed for a correlation of surface species and reactivity and thereby the identification of real intermediates. On the basis of this, a reaction mechanism is proposed. In this mechanism, methyl formate is unlikely to be an intermediate in the selective MSR reaction to CO_2 and H_2. Water converts stable bridging- and bidentate formates into more reactive, monodentate formates, which react either with adsorbed methoxy to MFO (more slowly) or with OH groups supplied by H_2O to CO_2 and H_2 (faster). A new formate species characterized by a band at 1570 cm^{-1} was resolved only in the phase-sensitive detection by its different kinetic response and is assigned to a formate bridging over Ga(o)-Ga(t). This site may constitute the reactive oxygen site on Ga_2O_3 produced upon formation of the IMC Pd_2Ga.

Overall, the Ga_2O_3 support plays an essential role in MSR. Formation of intermetallic Pd_2Ga by high-temperature reduction is required for achieving high MSR selectivity by slowing down unwanted methanol decomposition to CO on Pd as well as for producing the reactive oxygen sites. Our results suggest that the reaction sequence predominantly proceeds on the Ga_2O_3 that is modified by the high temperature reduction, and is promoted by the presence of the Pd_2Ga particles which may act as a sink for atomic hydrogen.

■ ASSOCIATED CONTENT

Supporting Information

FTIR spectra of the temperature-programmed surface reaction of methanol on Ga_2O_3 reduced at 673 K. This material is available free of charge via the Internet at http://pubs.acs.org.

■ AUTHOR INFORMATION

Corresponding Author

*Phone: +43 1 58801 165110. Fax: +43 1 58801 16599. E-mail: karin.foettinger@tuwien.ac.at.

Notes

The authors declare no competing financial interest.

■ ACKNOWLEDGMENTS

The COST Action CM0904 "Intermetallic compounds as catalysts in methanol steam reforming" has fostered this publication.

■ REFERENCES

(1) Olah, G. A. *Angew. Chem., Int. Ed.* **2005**, *44*, 2636−2639.
(2) Trimm, D. L.; Onsan, Z. I. *Catal. Rev.* **2001**, *43*, 31−84.
(3) Palo, D. R.; Dagle, R. A.; Holladay, J. D. *Chem. Rev.* **2007**, *107*, 3992−4021.
(4) Sá, S.; Silva, H.; Brandão, L.; Sousa, J. M.; Mendes, A. *Appl. Catal., B* **2010**, *99*, 43−57.
(5) Behrens, M.; Armbrüster, M. In *Catalysis: Alternative Energy Generation*; Guczi, L., Erdôhelyi, A., Eds.; Springer: New York, 2010; p 175.
(6) Cheng, X.; Shi, Z.; Glass, N.; Zhang, L.; Zhang, J. J.; Song, D. T.; Liu, Z. S.; Wang, H. J.; Shen, J. *J. Power Sources* **2007**, *165*, 739−756.
(7) Conant, T.; Karim, A.; Lebarbier, V.; Wang, Y.; Girgsdies, F.; Schlögl, R.; Datye, A. *J. Catal.* **2008**, *257*, 64−70.
(8) Iwasa, N.; Mayanagi, T.; Ogawa, N.; Sakata, K.; Takezawa, N. *Catal. Lett.* **1998**, *54*, 119−123.
(9) Penner, S.; Lorenz, H.; Jochum, W.; Stöger-Pollach, M.; Wang, D.; Rameshan, C.; Klötzer, B. *Appl. Catal., A* **2009**, *358*, 193−202.
(10) Haghofer, A.; Föttinger, K.; Girgsdies, F.; Teschner, D.; Knop-Gericke, A.; Schlögl, R.; Rupprechter, G. *J. Catal.* **2012**, *286*, 13−21.
(11) Haghofer, A.; Föttinger, K.; Nachtegaal, M.; Armbrüster, M.; Rupprechter, G. *J. Phys. Chem. C*, **2012**, accepted. DOI: 10.1021/jp3061224.
(12) Rameshan, C.; Stadlmayr, W.; Penner, S.; Lorenz, H.; Mayr, L.; Hävecker, M.; Blume, R.; Rocha, T.; Teschner, D.; Knop-Gericke, A.; Schlögl, R.; Zemlyanov, D.; Memmel, N.; Klötzer, B. *J. Catal.* **2012**, *290*, 126−137.
(13) Rameshan, C.; Stadlmayr, W.; Weilach, C.; Penner, S.; Lorenz, H.; Hävecker, M.; Blume, R.; Rocha, T.; Teschner, D.; Knop-Gericke, A.; Schlögl, R.; Memmel, N.; Zemlyanov, D.; Rupprechter, G.; Klötzer, B. *Angew. Chem., Int. Ed.* **2010**, *49*, 3224−3227.
(14) Rameshan, C.; Weilach, C.; Stadlmayr, W.; Penner, S.; Lorenz, H.; Hävecker, M.; Blume, R.; Rocha, T.; Teschner, D.; Knop-Gericke, A.; Schlögl, R.; Zemlyanov, D.; Memmel, N.; Rupprechter, G.; Klötzer, B. *J. Catal.* **2010**, *276*, 101−113.
(15) Smith, G.; Lin, S.; Lai, W.; Datye, A.; Xie, D.; Guo, H. *Surf. Sci.* **2011**, *605*, 750−759.
(16) Lorenz, H.; Jochum, W.; Klötzer, B.; Stöger-Pollach, M.; Schwarz, S.; Pfaller, K.; Penner, S. *Appl. Catal., A* **2008**, *347*, 34−42.
(17) Lorenz, H.; Penner, S.; Jochum, W.; Rameshan, C.; Klötzer, B. *Appl. Catal., A* **2009**, *358*, 203−210.
(18) Collins, S. E.; Baltanás, M. A.; Bonivardi, A. L. *J. Catal.* **2004**, *226*, 410−421.
(19) Jiang, C. J.; Trimm, D. L.; Wainwright, M. S.; Cant, N. W. *Appl. Catal., A* **1993**, *93*, 245−255.
(20) Frank, B.; Jentoft, F. C.; Soerijanto, H.; Kröhnert, J.; Schlögl, R.; Schomäcker, R. *J. Catal.* **2007**, *246*, 177−192.
(21) Takezawa, N.; Iwasa, N. *Catal. Today* **1997**, *36*, 45−56.
(22) Lin, S.; Xie, D.; Guo, H. *ACS Catal.* **2011**, *1*, 1263−1271.
(23) Takahashi, K.; Takezawa, N.; Kobayashi, H. *Appl. Catal.* **1982**, *2*, 363−366.
(24) Collins, S.; Baltanás, M.; Bonivardi, A. *Appl. Catal., A* **2005**, *295*, 126−133.
(25) Baurecht, D.; Fringeli, U. *Rev. Sci. Instrum.* **2001**, *72*, 3782−3792.
(26) Urakawa, A.; Bürgi, T.; Baiker, A. *Chem. Eng. Sci.* **2008**, *63*, 4902−4909.
(27) Jochum, W.; Penner, S.; Föttinger, K.; Kramer, R.; Rupprechter, G.; Klötzer, B. *J. Catal.* **2008**, *256*, 268−277.
(28) Busca, G.; Rossi, P.; Lorenzelli, V.; Benaissa, M.; Travert, J.; Lavalley, J. *J. Phys. Chem.* **1985**, *89*, 5433−5439.
(29) Kähler, K.; Holz, M. C.; Rohe, M.; Strunk, J.; Muhler, M. *ChemPhysChem* **2010**, *11*, 2521−2529.
(30) Collins, S. E.; Briand, L. E.; Gambaro, L. A.; Baltanás, M. A.; Bonivardi, A. L. *J. Phys. Chem. C* **2008**, *112*, 14988−15000.
(31) Turco, M.; Bagnasco, G.; Costantino, U.; Marmottini, F.; Montanari, T.; Ramis, G.; Busca, G. *J. Catal.* **2004**, *228*, 56−65.
(32) McInroy, A. R.; Lundie, D. T.; Winfield, J. M.; Dudman, C. C.; Jones, P.; Lennon, D. *Langmuir* **2005**, *21*, 11092−11098.
(33) Busca, G.; Elmi, A.; Forzatti, P. *J. Phys. Chem.* **1987**, *91*, 5263−5269.
(34) Bertarione, S.; Scarano, D.; Zecchina, A.; Johánek, V.; Hoffmann, J.; Schauermann, S.; Libuda, J.; Rupprechter, G.; Freund, H.-J. *J. Catal.* **2004**, *223*, 64−73.
(35) Bermudez, V. *Chem. Phys.* **2006**, *323*, 193−203.
(36) Calatayud, M.; Collins, S.; Baltanás, M.; Bonivardi, A. *Phys. Chem. Chem. Phys.* **2009**, *11*, 1397−1405.
(37) Lear, T.; Marshall, R.; Lopez-Sanchez, J. A.; Jackson, S. D.; Klapotke, T. M.; Bäumer, M.; Rupprechter, G.; Freund, H.-J.; Lennon, D. *J. Chem. Phys.* **2005**, *123*, 174706−174713.
(38) Gates, J.; Kesmodel, L. *J. Catal.* **1983**, *83*, 437−445.
(39) Rebholz, M.; Kruse, N. *J. Chem. Phys.* **1991**, *95*, 7745−7759.
(40) Borasio, M.; de la Fuente, O.; Rupprechter, G.; Freund, H.. *J. Phys. Chem. B* **2005**, *109*, 17791−17794.
(41) Morkel, M.; Kaichev, V.; Rupprechter, G.; Freund, H.; Prosvirin, I.; Bukhtiyarov, V. *J. Phys. Chem. B* **2004**, *108*, 12955−12961.
(42) Ouyang, F.; Kondo, J. N.; Maruya, K.; Domen, K. *J. Phys. Chem. B* **1997**, *101*, 4867−4869.

(43) Ota, A.; Armbrüster, M.; Behrens, M.; Rosenthal, D.; Friedrich, M.; Kasatkin, I.; Girgsdies, F.; Zhang, W.; Wagner, R.; Schlögl, R. *J. Phys. Chem. C* **2011**, *115*, 1368−1374.
(44) Yamada, M.; Ide, Y.; Tone, K. *Appl. Surf. Sci.* **1993**, *70*−*71*, 531−535.
(45) Akhter, S.; Cheng, W.; Lui, K.; Kung, H. *J. Catal.* **1984**, *85*, 437−456.
(46) Jung, K.; Joo, O. *Bull. Korean Chem. Soc.* **2002**, *23*, 1135−1138.
(47) Papavasiliou, J.; Avgouropoulos, G.; Ioannides, T. *Appl. Catal., B* **2009**, *88*, 490−496.
(48) Shido, T.; Iwasawa, Y. *J. Catal.* **1991**, *129*, 343−355.
(49) Bandara, A.; Kubota, J.; Onda, K.; Wada, A.; Kano, S.; Domen, K.; Hirose, C. *J. Phys. Chem. B* **1998**, *102*, 5951−5954.
(50) Kovnir, K.; Armbrüster, M.; Teschner, D.; Venkov, T.; Szentmiklósi, L.; Jentoft, F.; Knop-Gericke, A.; Grin, Y.; Schlögl, R. *Surf. Sci.* **2009**, *603*, 1784−1792.
(51) Busca, G.; Lorenzelli, V. *Mater. Chem.* **1982**, *7*, 89−126.
(52) Collins, S. E.; Baltanás, M. A.; Bonivardi, A. L. *J. Phys. Chem. B* **2006**, *110*, 5498−5507.
(53) Gonzalez, E.; Jasen, P.; Juan, A.; Collins, S.; Baltanás, M.; Bonivardi, A. *Surf. Sci.* **2005**, *575*, 171−180.